THE ASTROPHYSICAL JOURNAL, 450:435–440, 1995 September 1
© 1995. The American Astronomical Society. All rights reserved. Printed in U.S.A.

THE RADIO PROPERTIES OF SOLAR ACTIVE REGION SOFT X-RAY TRANSIENT BRIGHTENINGS

S. M. WHITE,[1] M. R. KUNDU,[2] T. SHIMIZU,[3] K. SHIBASAKI,[2] AND S. ENOME[2]
Received 1994 November 30; accepted 1995 March 13

ABSTRACT

We present the results of a search for radio emission from active-region transient brightenings identified in *Yohkoh* soft X-ray telescope observations of active region AR 7260. We present detailed observations of four events in which 17 GHz radio emission is clearly detected in observations by the Nobeyama radioheliograph. The time profiles of the 17 GHz data are very similar to those of the soft X-ray fluxes, and the 17 GHz flux is very close to that expected from plasma with the temperature and emission measure derived for the soft X-ray–emitting material from filter ratios. No impulsive nonthermal radio emission was detected from any of the four events, although each was at least *GOES* class B1 in soft X-rays. Weak hard X-rays may have been detected by *GRO*/BATSE from the strongest of the events, but not from two others. These negative results leave open the possibility that there is a difference between active region transient brightenings and solar flares, in that the former do not convert a significant amount of the released energy into accelerated electrons. However, confirmation of this hypothesis will require a larger sample of events.

Subject headings: Sun: activity — Sun: corona — Sun: radio radiation — Sun: X-rays, gamma rays

1. INTRODUCTION

One of the profound discoveries made by the Japanese solar-dedicated satellite *Yohkoh* is the dynamic nature of the solar corona, revealed by the numerous small flarelike brightenings detected in active regions by the soft X-ray telescope (SXT). The excellent sensitivity, high spatial resolution, low scattering, and high time resolution of SXT enabled it to detect these small events. Such small energy releases had long been suspected to occur and were thought possibly to play a role in coronal heating, but their nature and properties were completely unknown prior to the *Yohkoh* observations.

In soft X-rays, these energy releases take the form of sudden brightenings of magnetic loops in the corona above an active region (hence the name "active region transient brightenings," or ARTBs). The brightenings last 5–20 minutes, may occur on single or multiple loops, and frequently show a Y morphology as if two loops were in contact (Shimizu et al. 1992, 1994). Shimizu (1993) has shown that their characteristics may differ from one region to another, and Shimizu (1994) has discussed their possible contribution to coronal heating based on the distribution of energy releases detected by SXT in the range 10^{25}–10^{29} ergs.

The relationship of the brightenings to other coronal energy releases such as (the much larger) flares and filament eruptions is not yet clear. More can be learned about the physical nature of these brightenings by studying their properties at other wavelengths. Tsuneta & Lemen (1993) noted that ARTBs can be seen by the soft X-ray detectors of the *GOES* satellites, and that their properties as measured by *GOES* are similar to those of the hard X-ray "microflares" discussed by Lin et al. (1984). Tsuneta & Lemen (1993) therefore suggested that ARTBs might be the soft X-ray counterparts of hard X-ray microflares. If this is the case, it would also demonstrate that the mechanism which is responsible for the energy release seen as an ARTB can generate hard X-rays, just as a solar flare does. However, as yet no hard evidence for this hypothesis has been reported.

In this paper we combine radio observations from the Nobeyama 17 GHz Radioheliograph (NRH) and hard X-ray observations from the *Compton Gamma Ray Observatory* (*CGRO*) with data from *Yohkoh*/SXT, in order to study the properties of ARTBs at wavelengths other than soft X-rays, and to compare them with solar flares. An important aspect of this study is the availability of high-time-resolution images with excellent spatial resolution in both soft X-rays (SXT) and in radio (NRH). The ability to use spatial coincidence to ensure that phenomena at different wavelengths are truly associated avoids many of the uncertainties which often plague the correlation of weak phenomena such as these. This project started as an attempt to see if radio emission could be detected from ARTBs, and we have therefore concentrated on four of the brightest ARTBs identified by Shimizu (1993) in NOAA AR 7260. We discuss the data and its analysis in the following section, and present images of the ARTBs in the following section. We then go on to compare the radio properties of ARTBs with those of flares, and in particular address the question of whether there is evidence for nonthermal particle acceleration in ARTBs.

2. OBSERVATIONS

The ARTBs discussed were selected from a list of those occurring in NOAA AR 7260 (1992 August 15–20) compiled by Shimizu (1993). In order to determine the radio properties of ARTBs we use images from the Nobeyama radioheliograph (Japan), which has been carrying out routine operations at 17 GHz since 1992 June. Consisting of 84 × 80 cm dishes in a T-shaped array (east–west dimension of 490 m), it can make snapshot images of the whole solar disk with a spatial resolution of 18″ every 50 ms (Nakajima et al. 1994). The images are calibrated absolutely against the temperature of the

[1] Department of Astronomy, University of Maryland, College Park MD 20742.
[2] Nobeyama Radio Observatory, National Astronomical Observatory, Minamisaku, Nagano 384-13, Japan.
[3] Institute of Astronomy, University of Tokyo, Mitaka, Tokyo 181, Japan.

© American Astronomical Society • Provided by the NASA Astrophysics Data System

quiet solar disk at 17 GHz, known to be 10,000 K. Due to the large number of baselines involved, a single image from NRH presently requires 3 minutes of processing on a mini-supercomputer. Due to this requirement it is not usually feasible to make images at full time resolution for the whole duration of an event, and here we have made images at selected times centered on the peak time of the ARTB as determined by SXT.

Yohkoh is a Japanese satellite carrying instruments dedicated to solar observations (Ogawara et al. 1991). The SXT (Tsuneta et al. 1991) uses grazing-incidence optics to form images on a 1024 × 1024 pixel CCD in the energy range 0.25–4 keV; a number of filters can be placed in the optical path to select different photon energy ranges. The pixel size is 2".5. The events discussed here did not trigger the flare mode of operation of *Yohkoh*, so images are available approximately every 40 s, in the thick and thin Al filters, alternately.

The hard X-ray data used in this study are obtained from the four discriminator channels of the large-area detectors of the Burst and Transient Source Experiment (BATSE; principal investigator, Gerry Fishman, NASA/MSFC) on the *CGRO*. The discriminator data (DISCLA) consist of 1.024 s, accumulations in energy channels with the nominal ranges 25–50 keV, 50–100 keV, 100–300 keV, and 300 keV–1.0 MeV. Each detector has an area of 2000 cm^2 (the effective area for a given flare is reduced by projection onto the Sun-Earth line). These detectors are easily capable of detecting flares whose soft X-ray counterparts may be as small as B1 in the *GOES* soft-X-ray classification scheme. Light curves displayed below have had a long-term linear trend removed.

Based on a preliminary inspection of radio and soft X-ray data for roughly 10 ARTBs of varying sizes, we selected for more detailed analysis four events in which 17 GHz radio emission appeared to occur cospatially and approximately simultaneously with the soft X-ray emission. This selection did not involve detailed comparison of light curves or locations, and the four events presented in this paper are the only ones we have studied in detail, so no additional bias was introduced in the selection apart from the apparent spatial overlap. However, this paper is not intended to be a study of the radio emission of an unbiased sample of ARTBs, which will be carried out in a later paper, but rather a look at the properties of several events detected with good signal-to-noise ratio.

3. COMPARISON OF RADIO AND SOFT X-RAY IMAGES

The four ARTBs discussed here (one on August 17, two on August 19, one on August 20) are listed in Table 1. Radio and soft X-ray images of the four are shown in Figure 1 (Plate 10). In all cases the radio emission associated with the ARTB was substantially weaker than the steady radio emission associated with the active region itself, which was particularly strong in this region (Shibasaki et al. 1994). By contrast, the soft X-ray brightenings were generally the brightest features in the soft X-ray images of the region. To separate the weak emission associated with the ARTBs from the much stronger emission associated with the active region, the analysis is greatly aided by the use of difference images, in which the active-region emission has been subtracted out using a prebrightening image. In Figure 1 the left-hand column shows the prebrightening soft X-ray image from SXT data (gray scale, square root intensity display; all displayed images are taken through the thin Al filter) with contours of a prebrightening 17 GHz radio image overlaid. The times of the NRH and SXT images are generally not quite coincident and are shown in each panel. In each row the second and third panels represent difference images (see caption).

Co-alignment of the 17 GHz and soft X-ray images was carried out by comparing the extended thermal emission associated with the active region, which is visible in both images (Enome et al. 1994). The co-alignment is carried out on the prebrightening images. No additional co-alignment of the radio images relative to the soft X-ray images is carried out once established for the prebrightening images, so the coincidence of the radio and SXT sources in the third column of the panels is independent confirmation of the original co-alignment. We estimate an uncertainty of 5" in the alignment of radio and soft X-ray images.

The typical level of residuals obtained in the subtraction of SXT images is generally quite small, as can be seen in the second column of panels where the bright extended emission from the active region is well subtracted. The level of residuals in the NRH images is also generally small, except where there is a very bright compact sunspot source over the leading spot in the group. This source, which was very highly polarized and represents the occurrence of 2000 G magnetic fields in the corona above the sunspot, was discussed by Shibasaki et al. (1994): it reached a peak brightness temperature of 6×10^5 K on August 15 and declined (in brightness temperature, not in size) thereafter, with peaks of $\sim 3 \times 10^5$ K on August 17–20. The large residual in the difference images associated with this strong source is due to two factors: small interferometer phase errors for such a compact source many times brighter than the rest of the region can result in small position shifts which, when differenced with another image, leave large residuals; and the fact that small-scale structure in current NRH data may shift uniformly by about 1 pixel (5") from one image to the next because of the technical difficulties in calibrating data from the small dishes needed to obtain full-disk images of the Sun at 17 GHz, i.e., the absolute positional information may be inconsistent from one image to the next by this amount. We remove this to a large extent by cross-correlating successive NRH images in a suitable intensity range and determining relative shifts down to $\frac{1}{8}$ of a pixel, but the accuracy of this procedure is still a limiting factor in the residuals in difference images. At

TABLE 1

DATA FOR ACTIVE REGION TRANSIENT BRIGHTENINGS

Date (1992) (1)	*GOES* Level (2)	T_{SXT} (peak; K) (3)	EM_{SXT} (peak; cm^{-3}) (4)	17 GHz Flux (Predicted; sfu) (5)	17 GHz Flux (Observed; sfu) (6)
Aug 17 3:13.....	B1	5.7×10^6	1.9×10^{47}	0.22	0.67
Aug 19 2:08.....	B1	6.8×10^6	2.8×10^{47}	0.30	0.41
Aug 19 4:09.....	B4	7.5×10^6	8.1×10^{47}	0.83	0.39
Aug 20 6:10.....	B1	6.8×10^6	3.4×10^{47}	0.36	0.20

© American Astronomical Society • Provided by the NASA Astrophysics Data System

the location of the bright peak over the leading sunspot in the NRH images the residual in the difference maps may be as high as 6×10^4 K. By contrast, in regions of the (undifferenced) NRH maps where there is smooth active-region emission at a level of up to 5×10^4 K, the residual in the difference images is typically less than 2000 K. Since the four ARTBs discussed here are all well away from the sunspot source, the large residuals there (visible in the right-hand portion of each panel in the third column) do not affect our analysis at all. An additional diagnostic of the presence of artifacts due to incorrect alignment of the two images used to form a difference image is the fact that usually this produces positive and negative features in the difference image, of roughly equal strength, as may be seen in the sunspot residuals, whereas the features associated with the ARTBs are all uniformly positive in the difference images and are the brightest features present apart from the sunspot residuals.

For quantitative analysis of the ARTBs we measured the fluxes in the available sequences of radio and SXT images (with the thin Al filter) by integrating over the smallest region of each image which contains the ARTB in both radio and soft X-rays. The resulting SXT fluxes are in units of "data number" (DN) s^{-1}, while the 17 GHz fluxes are converted from brightness temperature to solar flux units (sfu) using standard formulae. We estimated the uncertainties in the resulting fluxes by summing over a region of similar size in the portion of the subtracted images corresponding to the bright extended active-region emission. The results are rms values of approximately 5000 DN s^{-1} in the SXT fluxes and 0.05 sfu in the 17 GHz fluxes, although the uncertainties vary somewhat from case to case. Figures 2–5 show the resulting time profiles of the four ARTBs. In each case the *GOES* soft X-ray measurements are also plotted. *CGRO*/BATSE hard X-ray data are also available for the first three events and 25–50 keV count rates (binned to 4.1 s time resolution and with a linear trend removed) are also plotted in Figures 2–4, although in the case of Figure 3 *CGRO* was in the Earth's shadow until 02:07 UT, which is about the start time of the brightening. The data plotted are "background" data, and contain artifacts such as sudden jumps which are clearly instrument- and background-related.

We now discuss the details of each event in turn.

3.1. *1992 August 17 UT 3:15*

This ARTB is particularly interesting because it shows two spatially separated brightenings which have identical temporal behavior. At this stage of the development of AR 7260 (see, e.g., Leka et al. 1994), magnetic flux was emerging in two locations: to the northeast of the dominant leading spot (the brightest radio source in the top left panel of Fig. 1), and in the trailing (eastern) end of the region. This ARTB has brightenings in both of these locations (*middle panel, top row*, Fig. 1), and their time profiles are very similar (Fig. 2). Both of the soft X-ray brightenings appear to have counterparts in the 17 GHz images (*right panel*), and the residual of the bright sunspot source (southwestern source in the right panel) may also be seen. The eastern 17 GHz source does not lie exactly over its soft X-ray counterpart, but rather about 10″ to the south. The 17 GHz time profile matches that of the western brightening very well. Since the resolution of the radio images is about 10″, we are uncertain whether the offset is significant.

The soft X-ray sources are both elongated and may represent isolated loops, with the western source both much brighter and much longer than the eastern (Fig. 2). In the initial

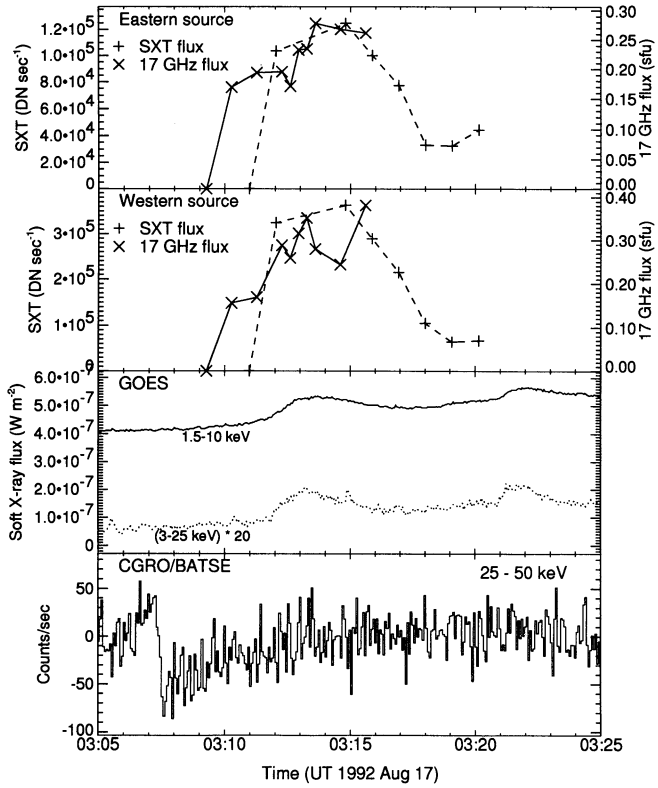

FIG. 2.—The time profile of the transient brightenings in AR 7260 at 3:15 UT on 1992 August 17. Since this event shows two well-separated brightenings, we have plotted their time profiles separately (*top two panels*). The SXT (thin Al filter) and 17 GHz fluxes are calculated by summing appropriate areas in the images. The scales for the SXT fluxes are given on the left-hand axes in the two upper panels, and the scales for the 17 GHz fluxes are given on the right-hand axes. The third panel shows the *GOES* 1.5–10 keV and 3–25 keV fluxes (nonimaging data) at 3 s time resolution on a linear scale; the 3–25 keV flux has been multiplied by 20 to show it on the same scale as the 1.5–10 keV flux. The fourth panel shows the 25–50 and 100–300 keV hard X-rays measured by the *CGRO*/BATSE detectors: these light curves have been binned to 4.096 s resolution and have had a linear long-term trend removed.

brightening (3:12:02 UT) the western source is saturated in the SXT image and suggests the presence of two parallel loops. One of these is the loop seen in Figure 1, while the brighter loop appears to have the same footpoints but lies higher in the corona. The western brightening occurs at a location which is already bright in the 3:10:58 image, whereas the eastern brightening occurs in a region which is not noticeably bright in the prebrightening image. There is no sign of any connection between the eastern and western sources in the SXT difference images, so it may just be coincidental that they show identical time evolution, or else some larger scale event is responsible for their simultaneous brightening. The radio emission from the two appears to have similar characteristics.

3.2. *1992 August 19 UT 2:08*

In the two days between the first and second ARTBs we discuss, AR 7260 has changed dramatically. The bright (in soft X-rays) region northeast of the leading spot has moved further eastward relative to the leading spot, and the trailing portion of the region has become much brighter (left panel, second row, Fig. 1). The ARTB occurs in the southernmost section of the trailing portion (eastern end) of the active region, and appears to involve both the prominent "S"-shaped loop which is

© American Astronomical Society • Provided by the NASA Astrophysics Data System

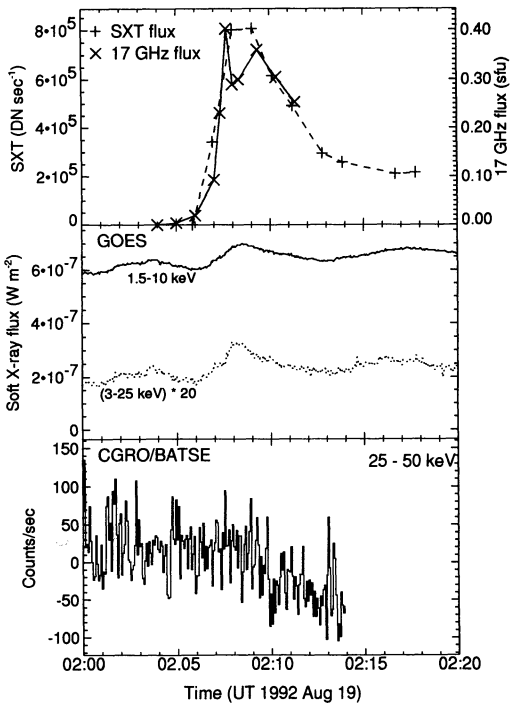

FIG. 3.—The time profile of the transient brightening in AR 7260 at 2:08 UT on 1992 August 19. The SXT (thin Al filter) and 17 GHz fluxes are plotted together in the top panel. The second panel shows the *GOES* 1.5–10 keV and 3–25 keV fluxes (nonimaging data) at 3 s time resolution on a linear scale; the 3–25 keV flux has been multiplied by 20 to show it on the same scale as the 1.5–10 keV flux. The bottom panel shows the 25–50 and 100–300 keV hard X-rays measured by the *CGRO*/BATSE detectors; however, note that *CGRO* was occulted from the Sun by the Earth until 2:07 UT.

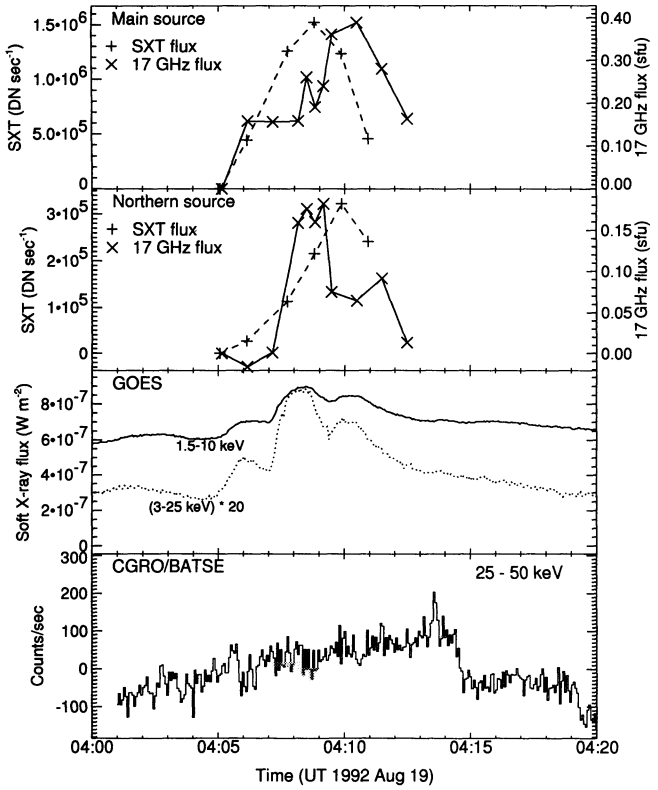

FIG. 4.—The time profile of the transient brightening in AR 7260 at 4:09 UT on 1992 August 19, in the same format as Fig. 2. Separate plots are given for the SXT and 17 GHz emission from the main (southern) source in the images and for the northern source (*top two panels*).

already bright in the first image (2:05:51), and a much more compact loop just south of it which was not bright in the first image. The latter is the brighter source in soft X-rays in the subsequent event. The radio source appears to encompass both locations where X-ray brightening is observed, and just as in soft X-rays the compact southern source is the brightest source of radio emission. The time profiles of the radio and soft X-ray emission match extremely well (Fig. 3), so that this appears to be a simple case in which the radio and soft X-rays come from the same location and display the same temporal behavior.

3.3. *1992 August 19 UT 4:09*

Over the intervening 2 hr since the previous ARTB, the soft X-ray emission at the same location has brightened considerably. This ARTB occurs in essentially the same location as the previous one, and again two loops appear to be involved. The soft X-ray images are dominated by a single, very compact brightening, which appears to be a very short ($\sim$15″) loop. However, a weak second loop is visible in the difference images and in the prebrightening image, apparently with one footpoint very close to the compact loop but with the other footpoint some 40″ to the north. The 17 GHz difference map shows two souces: one is coincident with the main soft X-ray brightening, while the other, much weaker, lies to the northwest. It is roughly coincident with the northern footpoint of the weaker loop seen in soft X-rays, and appears to be circularly polarized, although the source is sufficiently weak that we cannot make a useful estimate of the degree of polarization. The northern radio source shows a much more erratic time profile than the stronger southern radio source. Figure 4 shows the time profiles of the radio and soft X-ray emission from the main (southern) and northern sources separately: the radio and soft X-ray profiles are generally similar, but do not show the same detailed similarity as the other examples. The *GOES* profiles show three separate brightenings at the time of this event, but the SXT fluxes do not show such behavior: this may mean that the three brightenings in the *GOES* data occur at different locations, or else the cadence of the SXT images is not rapid enough to resolve the three brightenings in time.

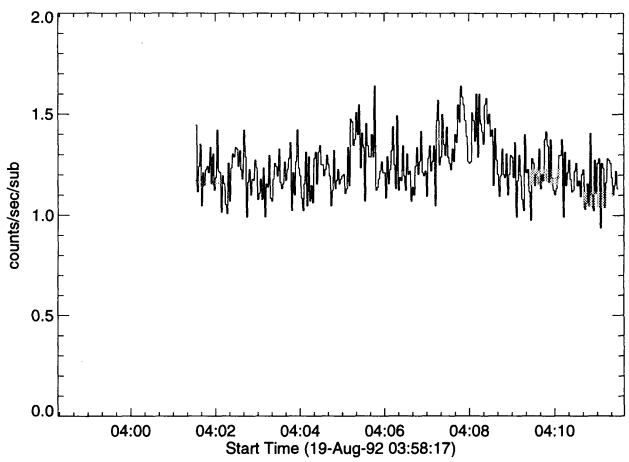

FIG. 5.—The time profile of the 14–23 keV hard X-ray emission detected by the HXT telescope on *Yohkoh* during the period of the transient brightening at 4:09 UT on 1992 August 19.

© American Astronomical Society • Provided by the NASA Astrophysics Data System

This is the only event in which there is some evidence for the detection of hard X-rays: between 4:05 and 4:06 there is a small peak at approximately 60 counts s^{-1} in the *CGRO* 25–50 keV count rate. This peak is so weak that its significance is questionable, but the Hard X-ray Telescope (HXT) on *Yohkoh* also detects a very weak excess of 14–23 keV hard X-rays at this time (Fig. 5), and consequently we believe it to be significant. HXT also indicates weak emission at 4:08, at the time of the second *GOES* peak, which is not seen in the *CGRO*/BATSE data.

3.4. *1992 August 20 UT 6:11*

AR 7260 has again changed dramatically in the SXT images in the 26 hr since the previous ARTB. The region is now dominated by a long "backbone" of emission connecting the trailing spots to a location just south of the leading spot. This ARTB again occurs at the southern edge of the trailing group of sunspots, in a location which is not bright in soft X-rays prior to the ARTB. It has the appearance of a compact loop, about 20″ long, and is the only one of the four examples in which only a single loop was apparently involved. In this case there is also a single compact radio source which is coincident with the soft X-ray brightening. The radio and soft X-ray time profiles are again strikingly similar (Fig. 6).

4. THE PROPERTIES OF THE TRANSIENT BRIGHTENINGS

Table 1 summarizes the properties of the four ARTBs discussed above. The second column gives the *GOES* level of the enhancement associated with the brightening. All the brightenings were observed with both thick and thin Al filters, and we have used the filter ratio to estimate the temperature and emission measure at the peak of each event. Since adjacent observations with the two filters are typically 30–40 s apart, there may be some changes between the two which will affect the resulting ratio, and consequently we regard the values for temperature and emission measure as only approximate. However, the derived temperatures are all 6–7 × 10^6 K, which is typical of ARTBs (Shimizu et al. 1992). Given the temperature and emission measure, it is straightforward to predict the radio flux which will be produced by thermal bremsstrahlung in the material producing the soft X-rays (e.g., Hudson & Ohki 1972), and this quantity is given in column (5). Finally, in column (6) we give the peak 17 GHz flux measured from the difference images. We note that, at *GOES* levels of at least B1, these four ARTBs are quite typical members of their class in their soft X-ray fluxes as well as in their soft X-ray morphology, temperatures, and temporal behavior (Shimizu et al. 1992; Shimizu 1993; Shimizu et al. 1994).

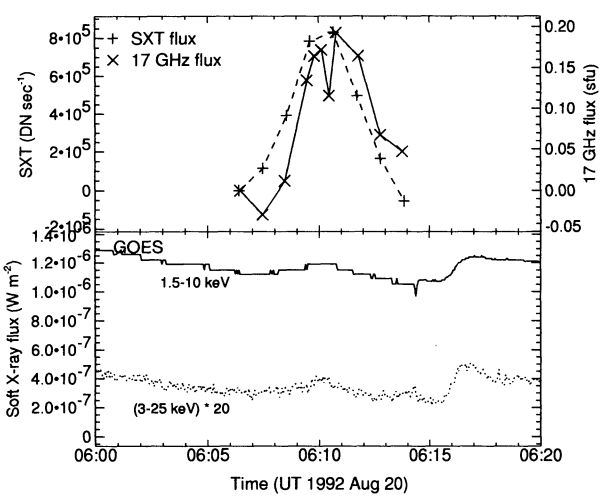

FIG. 6.—The time profile of the transient brightening in AR 7260 at 6:11 UT on 1992 August 20, in the same format as Fig. 3 with the exception that there are no *CGRO* data at the time of this event.

In general, the radio emission seems to match the time profile of the soft X-ray material well, with a nonimpulsive profile and durations of 5–10 minutes. We note from Table 1 that in all cases the radio emission predicted on the basis of thermal bremsstrahlung emission from the X-ray–emitting material is reasonably close to the peak flux actually observed. Given the uncertainties in both the radio measurements and the derived soft X-ray properties, this agreement suggests that thermal bremsstrahlung is the emission mechanism for the 17 GHz sources. The obvious alternative would be gyrosynchrotron emission from nonthermal electrons accelerated during the brightening, as occurs in solar flares. We can think of three simple tests for the presence of nonthermal electrons.

1. The presence of additional radio flux not explained by thermal bremsstrahlung. In impulsive solar flares at 17 GHz the nonthermal gyrosynchrotron emission is generally larger than the thermal bremmstrahlung emission (e.g., see examples in Takano et al. 1994; Nishio et al. 1994; Kundu et al. 1995), and we would expect to see a component of the radio emission more impulsive than the time profiles that Figures 2–6 display. Such impulsive emission is not seen, either in the imaging data used in Figures 2–6, which have limited temporal cadence and might have missed a very short impulsive spike, or in the NRH "correlation" plots which are available at 1 s resolution, are sensitive to compact sources such as nonthermal spikes, and can easily detect a flux of 0.2 sfu.

2. The presence of circular polarization in the radio emission. None of these events showed any circular polarization in the images, down to a detection level of 500 K in brightness temperature (note that we exclude the northern radio source in the third example, which was not coincident with bright soft X-ray emission and which we discuss further below). This implies a degree of polarization of less than 5%, which is more typical of thermal bremsstrahlung than of gyrosynchrotron emission.

3. The detection of nonthermal hard X-rays. As noted above, two of the events were well covered by the *CGRO*/BATSE detectors while a third was largely covered. Only the largest of the events (B4, 4:09 UT August 19) may have been detected in 25–50 keV hard X-rays by BATSE, or in 14–23 keV hard X-rays by HXT. BATSE is easily capable of detecting hard X-rays from *GOES*-class B1 flares (e.g., examples in Kundu et al. 1994; and R. A. Schwartz, private communication), although, for a given soft X-ray size, flares show a wide range of peak hard X-ray count rates so it is difficult to quantify this statement. The count rate of the only event detected is close to the detection limit of BATSE's detectors (Biesecker, Ryan & Fishman 1994). Thus, although we cannot make a quantitative statement in the absence of statistics on the distribution of BATSE count rates with *GOES* soft X-ray flare size, it is possible that these ARTBs are weak in hard X-rays compared with solar flares of similar soft X-ray sizes.

Recently Gopalswamy et al. (1994) have detected 15 GHz emission from soft X-ray brightenings in another active region using the Very Large Array (VLA). In their case several radio

© American Astronomical Society • Provided by the NASA Astrophysics Data System

brightenings occurred in the penumbra of a large sunspot, and were very highly circularly polarized (up to 100%), in contrast to the observations here which generally involved brightenings in loops away from sunspots and were unpolarized. Two of the VLA radio brightenings were spatially associated with soft X-ray brightenings, although the 15 GHz time profiles did not match the associated soft X-ray time profiles as closely as the brightenings presented here. The majority of the VLA radio brightenings were not associated with soft X-ray increases measured by *GOES*. The high degree of polarization in the VLA radio data and the association with the penumbra suggest that the radio emission in those cases was thermal gyroresonance emission (radiation at low harmonics of the gyrofrequency) in the strong magnetic fields low in the corona near the sunspot, although Gopalswamy et al. (1994) could not rule out the possibility that the emission was nonthermal gyrosynchrotron emission by accelerated electrons (which generally has degrees of polarization much lower than 100%). Consistent with the thermal interpretation is the fact that they did not observe radio emission from the whole loop which brightened in soft X-rays, but only from the footpoint anchored in the penumbra, i.e., from the region of strongest magnetic field in the loop. Total 15 GHz fluxes associated with the brightenings were much smaller than in our cases, as were the soft X-ray brightenings themselves. If we accept the argument that the radio emission in those cases was thermal gyroresonance emission, then they also failed to detect any clear signature of impulsive radio emission due to nonthermal accelerated particles associated with the ARTBs.

The weak northern radio source detected in the August 19 4:09 UT event here, which was circularly polarized, seen only at one end of a weak soft X-ray loop and varied erratically in time, occurred at a location which was polarized in the prebrightening image. Such polarized sources in active region images at 17 GHz are generally the locations of strong sunspots, and inspection of the optical images indicates that this is true of this source also. None of the other ARTB radio sources occurred at locations which were polarized in the prebrightening images, so this suggests that the weak northern radio source may have been a gyroresonance source similar to those detected by Gopalswamy et al. (1994). Due to the additional opacity provided by the gyromagnetic resonance, such sources will be much brighter relative to the level of soft X-ray emission at their location than the pure thermal free-free radio sources.

5. CONCLUSIONS

Radio emission at 17 GHz is clearly detected from ARTBs. The radio data show a time profile very similar to that of the soft X-ray emission, and a peak flux which matches that expected from thermal bremsstrahlung in a plasma with the derived (from SXT filter ratios) temperature (typically 6–7 $\times$ 10^6 K) and emission measure of the soft X-ray-emitting material.

No evidence for nonthermal radio emission at 17 GHz was detected from any event, even though in a typical impulsive solar flare we would expect the nonthermal emission at 17 GHz to be stronger than any thermal free-free component. Weak hard X-rays may have been detected from the strongest of the brightenings, but not from two other events. These results leave open the possibility that there exist important differences between ARTBs and (at least impulsive) solar flares, in that acceleration of electrons to nonthermal energies seems to be greatly reduced in ARTBs compared to impulsive solar flares. However, this is a small sample of events and the result does not have the confidence of a large statistical survey to support it.

We have selected events in which radio emission was clearly detected, in order to establish the radio properties of ARTBs. It is possible that nonthermal radio emission is present but relatively weak at 17 GHz, due either to a low turnover frequency in the radio spectrum, or to a particularly steep radio spectrum at high frequencies (corresponding to a very soft nonthermal electron energy spectrum). In this case such weak nonthermal emission from ARTBs might be detectable by the VLA at a frequency lower than 17 GHz. In the observations by Gopalswamy et al. (1994), which were not designed for such a study, there was temporal overlap between 15 GHz observations and SXT ARTB detections sufficient to address this question for only one event, which did not show such emission, so this question remains for future observations to answer.

We thank T. Kosugi for his valuable comments and suggestions. Support for this work at the University of Maryland was received from NASA grant NAG-W-1541 and NSF grants ATM 90-19893 and ATM 93-16972. This work was initiated while M. R. K. was the guest of the Nobeyama Radioheliograph group, and he and S. M. W. thank the whole group, and particularly S. Enome, K. Shibasaki, and H. Nakajima, for their generous hospitality during their visits.

This research has made use of data obtained through the *CGRO* BATSE Solar Flare Data Archive maintained by the Solar Data Analysis Center at NASA/Goddard Space Flight Center and providd by the BATSE team headed by Gerald Fishman. We thank Richard Schwartz for his assistance in obtaining BATSE data for periods outside cataloged flare entries.

REFERENCES

Biesecker, D. A., Ryan, J. M., & Fishman, G. J. 1994, in High Energy Solar Phenomena: A New Era of Spacecraft Measurements, ed. J. Ryan & W. T. Vestrand (AIP Conf. Proc. 294), 199
Enome, S., et al. 1994, PASJ, 46, L27
Gopalswamy, N., Payne, T. E. W., Schmahl, E. J., Kundu, M. R., Lemen, J. R., Strong, K. T., Canfield, R. C., & de La Beaujardiere, J. 1994, ApJ, 437, 522
Hudson, H. S., & Ohki, K. 1972, Sol. Phys., 23, 155
Kundu, M. R., White, S. M., Gopalswamy, N., & Lim, J. 1994, ApJS, 90, 599
Kundu, M. R., White, S. M., Nitta, N., Shibasaki, K., Enome, S., Bruner, M., Sakao, T., & Kosugi, T. 1995, ApJ, submitted
Leka, K. D., van Driel-Gesztelyi, L., Nitta, N., Canfield, R. C., Mickey, D. L., Sakurai, T., & Ichimoto, K. 1994, Sol. Phys., 155, 301
Lin, R. P., Schwartz, R. A., Kane, S. R., Pelling, R. M., & Hurley, K. C. 1984, 283, 421
Nishio, M., et al. 1994, PASJ, 46, L11
Nakajima, H., et al. 1994, Proc. IEEE, 82, 705
Ogawara, Y., Takano, T., Kato, T., Kosugi, T., Tsuneta, S., Watanabe, T., Kondo, I., & Uchida, Y. 1991, Sol. Phys., 136, 1
Shibasaki, K., et al. 1994, PASJ, 46, L17
Shimizu, T. 1993, in Proc. of 2nd Japan-China Seminar on Solar Physics, ed. T. Sakurai et al. (Tokyo: NAOJ), 193
———. 1994, in Proc. Kofu Symposium on a New Look at the Sun, ed. S. Enome & T. Hirayama (Nobeyama: Nobeyama Radio Observatory), 61
Shimizu, T., Tsuneta, S., Acton, L. W., Lemen, J. R., Ogawara, Y., & Uchida, Y. 1994, AJ, 422, 906
Shimizu, T., Tsuneta, S., Acton, L., Lemen, J. R., & Uchida, Y. 1992, PASJ, 44, L147
Takano, T., et al. 1994, PASJ, 46, L21
Tsuneta, S., et al. 1991, Sol. Phys., 136, 37
Tsuneta, S., & Lemen, J. R. 1993, in Physics of Solar and Stellar Coronae, ed. J. F. Linsky & S. Serio (Dordrecht: Kluwer), 113

© American Astronomical Society • Provided by the NASA Astrophysics Data System